https://doi.org/10.5194/wcd-2021-69
Preprint. Discussion started: 19 October 2021

Weather and Climate Dynamics Discussions
Open Access
EGU

Past Evolution and Recent Changes in Western Europe Large-scale Circulation

Antoine Blanc[1], Juliette Blanchet[1], and Jean-Dominique Creutin[1]
[1]Univ. Grenoble Alpes, CNRS, IRD, Grenoble INP, IGE, 38000 Grenoble, France
Correspondence: Antoine Blanc (antoine.blanc2@univ-grenoble-alpes.fr)

Abstract. Detecting trends in regional large-scale circulation (LSC) is an important challenge as LSC is a key driver of local weather conditions. In this work, we investigate the past evolution of Western Europe LSC based on the 500 hPa geopotential height fields from 20CRv2c (1851-2010), ERA20C (1900-2010) and ERA5 (1950-2010) reanalyses. We focus on the evolution of large-scale circulation characteristics using three atmospheric descriptors that are based on analogy – characterizing the geopotential shape stationarity and how well a geopotential shape is reproduced in the climatology – together with a non-analogy descriptor accounting for the intensity of the centers of action. These descriptors were shown relevant to study precipitation extremes and variability in the Northwestern Alps in previous studies. Even though LSC characteristics and trends are consistent among the three reanalyses after 1950, we find major differences between 20CRv2c and ERA20C from 1900 to 1950 in accordance with previous studies. Notably, ERA20C produces flatter geopotential shapes in the beginning of the 20th century and shows a reinforcement of the meridional pressure gradient that is not observed in 20CRv2c. We then focus on the recent changes in LSC from 1950 to 2019 using ERA5. We combine the four atmospheric descriptors with an existing weather pattern classification to study the recent changes in the main atmospheric influences over France and Western Europe (Atlantic, Mediterranean, Northeast, Anticyclonic). We show that little changes are found in Northeast circulations. However, we show that Atlantic circulations (zonal flows) tend to become more similar to known Atlantic circulations in winter. Anticyclonic conditions tend to become more stationary in summer – a change that can potentially affect summer heatwaves. Furthermore, Mediterranean circulations tend to become more stationary, more similar to known Mediterranean circulations and associated with stronger centers of action in autumn, which could have implications for autumn extreme precipitation in the Mediterranean-influenced regions of the Southwestern Alps.

1 Introduction

By defining the direction and intensity of airflow towards a given region, large-scale circulation (LSC) is a key driver of local weather conditions. Over the large scale, LSC variability over the Euro-Atlantic sector influences precipitation and temperature anomalies over Europe and the Mediterranean region. The North Atlantic Circulation (NAO) is the first mode of LSC variability over the North Atlantic and the only one remaining the entire year (Barnston and Livezey, 1987). In winter, a positive phase of NAO drives mild air temperature over Europe, positive precipitation anomalies over Northern Europe and negative precipitation anomalies over Southern Europe by increasing westerlies (Hurrell, 1995). Nevertheless, other modes of LSC variability better

https://doi.org/10.5194/wcd-2021-69
Preprint. Discussion started: 19 October 2021

Weather and Climate Dynamics Discussions
Open Access
EGU

explain precipitation variability in Central Europe, especially in the Alpine region which acts as a climatological barrier at the crossroad of different atmospheric influences (Auer et al., 2007; Beniston, 2005). In winter, a negative phase of the Euro-Atlantic blocking (EAB) is associated to wet conditions in the Northern flanks of the Alps (Quadrelli et al., 2001; Scherrer et al., 2016), while a negative phase of the East Atlantic/Western Russia pattern (EA/WR) is associated to wet conditions over the main Alpine range and Western Europe (Bartolini et al., 2009). Low pressure anomalies over the near Atlantic drive wet conditions from the Western Mediterranean basin to the Southern flanks of the Alps, while the Atlantic ridge pattern leads to wet conditions in the Northern flanks of the Alps and in the Eastern Mediterranean basin (Kotsias et al., 2019; Plaut and Simonnet, 2001). In terms of temperature, cold day frequency is increased over Central and Western Europe under Scandinavian blocking through easterlies, while it is decreased under zonal flows bringing mild air from the Atlantic (Plaut and Simonnet, 2001).

Specific LSC patterns also drive extreme weather events over Europe and the Mediterranean region, including extreme precipitation (Giannakaki and Martius, 2016), floods (Stucki et al., 2012), extreme snowfall (Scherrer and Appenzeller, 2006), or heatwaves (Jézéquel et al., 2018). Extreme precipitation in the Western Mediterranean basin, Southwestern Europe, and in the southern slopes of the Alps mainly occur in autumn and they are associated with low pressure systems from the Atlantic to the Iberic Peninsula driving southwesterlies and strong southerly flows (Blanchet et al., 2021b; Horton et al., 2012; Mastrantonas et al., 2021; Plaut et al., 2001). Extreme precipitation in the Northwestern, Northern and Central Alps are associated with low amplitude through over the UK, zonally oriented flows and East Atlantic ridge driving southwesterlies-to-northwesterlies towards the region (Blanchet et al., 2021b; Giannakaki and Martius, 2016; Horton et al., 2012; Plaut et al., 2001). Over Central Europe, summer floods and extreme precipitation appear to be associated with quasi-stationary low pressure systems over the region (Grams et al., 2014; James et al., 2004) – the extreme nature of these phenomena being related to the extremeness in several atmospheric predictors (Kašpar and Müller, 2014; Müller et al., 2009). The probability of extreme precipitation events over Europe is decreased under a blocking high pressure system while it is increased southeast and southwest of the block (Lenggenhager and Martius, 2019). Blocking high pressure systems are also associated with temperature extreme over Europe, especially with warm spells in the Northern half of Europe and with spring cold spells in Western and Central Europe (Brunner et al., 2017; Pfahl and Wernli, 2012). The persistence of long-lasting blocking situations is pointed as a key ingredient driving European cold spells – by increasing cold air advection at the edges of the block –, and European warm spells – increasing solar radiation and air subsidence under the block (Brunner et al., 2017; Buehler et al., 2011; Jézéquel et al., 2018; Pfahl and Wernli, 2012). Over Western Europe, the occurrence of zonal circulations bringing mild subtropical air is also pointed as a synoptic circulation associated with warm extremes in winter (Jézéquel et al., 2017; Messori et al., 2017).

Knowing the link between LSC and local weather variability and extremes, changes in LSC may have significant impacts on local climate. Over the long run, increasing flood frequency in the European Alps during Holocene cold periods may be linked to a southward shift of the Hadley cell and a weakening of the Açores high allowing a southward shift of the Westerlies and meandering circulations (Glur et al., 2013; Wirth et al., 2013). More recently, the flood-rich period in Central Europe in the 19th century appears to be associated with a more zonal and southward-shifted circulation (Brönnimann et al., 2019). In the period 1948-2007, the seesaw between increasing precipitation frequency in Northern Europe and a decreasing precipitation frequency in Southern Europe in winter is well controlled by changes in atmospheric circulation (Vautard and Yiou, 2009).

https://doi.org/10.5194/wcd-2021-69
Preprint. Discussion started: 19 October 2021

Vautard and Yiou (2009) show that circulation changes poorly explain changes in surface climate in summer but they well control changes in winter, although this control seems to be weakening in the last 30 years. At a more local scale, decreasing autumn and winter precipitation from 1951 to 2000 in Southern France appears to be explained by a decrease in the occurrence of weather types driving precipitation over the region, while the increasing trend in Northeastern France is only partly explained by changes in weather type occurrence (Boé and Terray, 2008). In the British Isles, the decreasing trend in summer precipitation since 1850 appears to be related to more positive phases of the summer NAO pattern (Fig. 6b of Folland et al., 2009). Focusing on extremes, Horton et al. (2015) show that 44 % of the increase in summer hot extremes over Europe can be explained by an increase in the occurrence of blocking high pressure systems over Central Europe for the period 1979-2013. Iannuccilli et al. (2021) show that part of the increase in extreme precipitation over Central Italy in winter and spring can be explained by changes in occurrence of the circulation types. In the Southwestern Alps, the increasing extreme precipitation from 1958 to 2017 in autumn appear to be associated with a strengthening of the Mediterranean influence on extremes (Blanchet et al., 2021a, b).

The aforementioned studies dealing with trends in regional LSC mainly employ weather patterns classifications. However, part of the trend may also lie in changes in the characteristics within a given weather pattern – whether dynamical or thermodynamical –, as discussed in Boé and Terray (2008) and Iannuccilli et al. (2021). In this paper, we propose a contribution to fill this gap by employing four atmospheric descriptors that characterize the 500 hPa geopotential height field and that allow the consideration of dynamical trends within the main atmospheric influences. These descriptors were introduced in previous works, and they were shown to explain precipitation variability and extremes in the Northern French Alps (Blanc et al., 2021b; Blanchet and Creutin, 2020). They characterize i) the stationarity of a flow direction (celerity), ii) how well a flow direction is reproduced in the climatology (singularity, relative singularity), and iii) the intensity of the low and the high pressure systems (Maximum Pressure Difference). The four atmospheric descriptors are first employed to study the long-term evolution of Western Europe LSC from 1851 to 2010 using different reanalyses products. They are then combined with an existing weather pattern classification over the period 1950-2019 to address recent changes in the characteristics of the main atmospheric influences affecting Western Europe. Finally, the implications of these changes for local weather conditions are discussed.

2 Data

We use daily 500 hPa geopotential height fields over a $32° \times 16°$ region to represent Western Europe LSC (rectangle in Fig. 1a). The 500 hPa geopotential ranges from $4,800$ m to $6,100$ m, giving information about the location and the intensity of the low and the high pressure systems in the middle of the troposphere. We extracted the 500 hPa geopotential height from three different reanalyses covering different periods (Table 1).

We use the 20CRv2c reanalysis from NOAA-CIRES (Compo et al., 2011). 20CRv2c provides information about the state of the atmosphere since 1851 with an horizontal resolution of 2°. It only assimilates surface pressure observations using an ensemble Kalman Filter, and it is composed of 56 individual members that are equiprobable as well as a mean member. Sea

https://doi.org/10.5194/wcd-2021-69
Preprint. Discussion started: 19 October 2021

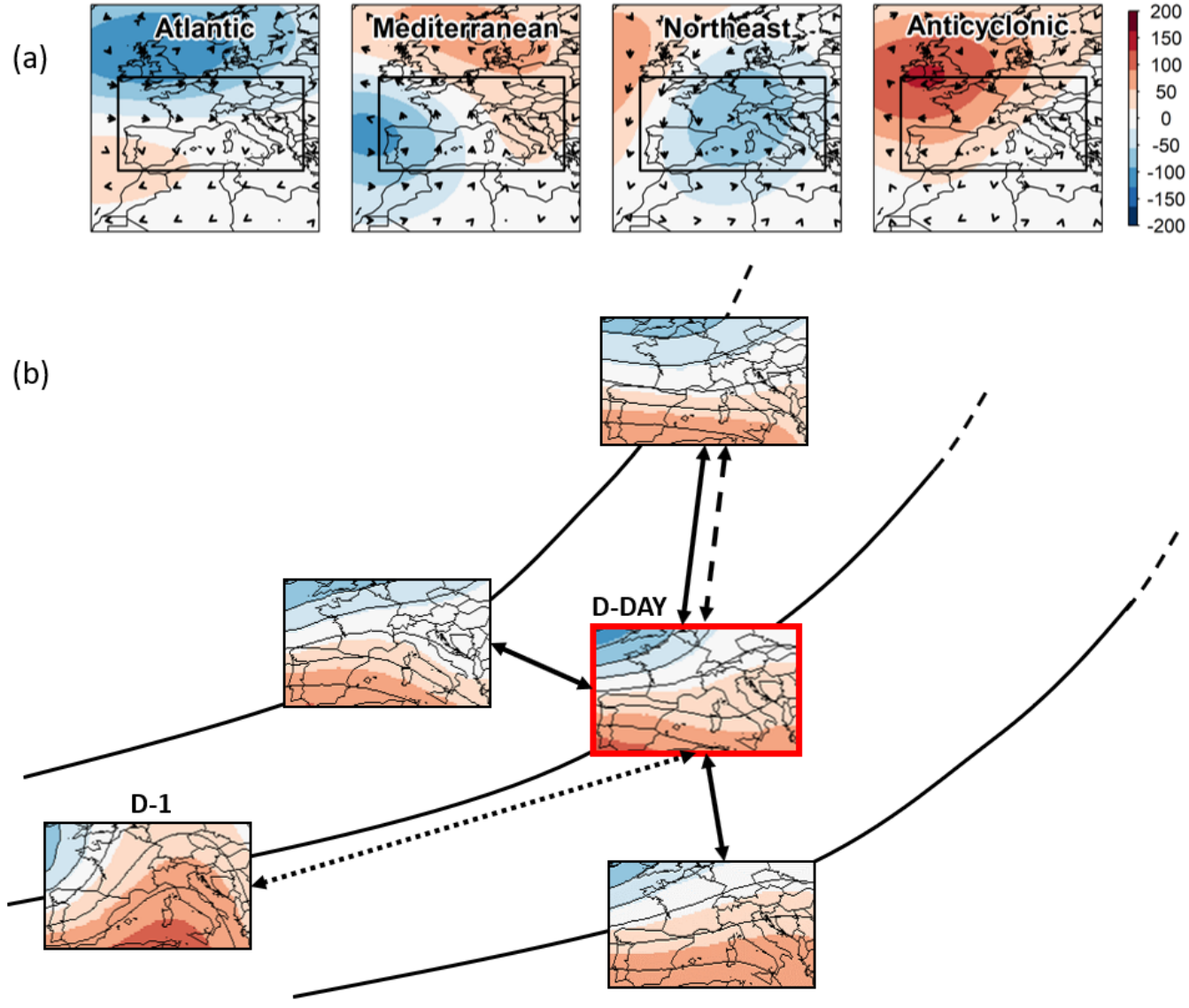

Figure 1. (a) Composite 500 hPa geopotential height anomalies (in meters) of the four atmospheric influences for the period 1950-2019. The arrows represent the wind anomalies at 500 hPa. In this study, the 500 hPa geopotential height is considered over the Western Europe region, represented by the black rectangle. (b) Schematic illustration of the atmospheric descriptors based on analogy. Each map represents the 500 hPa geopotential height field over Western Europe for a given day. Following days are represented on the same trajectory, but all trajectories are part of a single historical trajectory. The distance between each map represents here the difference in geopotential shapes/flow direction between individual days, using the Teweles-Wobus score. The celerity is the distance between a day D and the day before D-1 (dotted arrow). The singularity is the mean distance between a day D and its closest analogs (solid arrows; three analog days for illustration, but 111 analog days in our study). The relative singularity is the singularity normalized by the distance to the farthest analog (dashed arrow; third analog day for illustration, but 111th analog day in our study). The day D considered here is 12 December 1978.

https://doi.org/10.5194/wcd-2021-69
Preprint. Discussion started: 19 October 2021

Name	Institution	Period	Horizontal resolution	Model	Assimilated data
20CRv2c	NOAA-CIRES	1851-2014	$2° \times 2°$	GFS-2008ex	surface-input (surface pressure)
ERA20C	ECMWF	1900-2010	$1.125° \times 1.125°$	IFS-Cy38r1	surface-input (surface pressure, marine wind)
ERA5	ECMWF	1950-today	$0.25° \times 0.25°$	IFS-Cy41r2	full-input

Table 1. Main properties of the reanalyses used.

surface temperature and sea-ice distributions are used as boundary conditions. In this article, we use two individual members – arbitrary member 1 and member 2 – as well as the mean member to derive whether significant differences are observed between the individual and the mean members.

The twentieth century reanalysis ERA20C from ECMWF is also used (Poli et al., 2016). ERA20C provides a higher spatial resolution than 20CRv2c with a $1.125°$ grid, but it ranges over a shorter period (1900-2010). In addition to surface pressure, ERA20C also assimilates marine wind observations using a 4D-Var assimilation technique. ERA20C is single-member. It is forced by sea surface temperature, sea-ice cover, atmospheric composition and solar forcing.

Finally, we use the ERA5 reanalysis which is the most recent reanalysis product of ECMWF (Hersbach et al., 2020). ERA5 ranges over a more recent period (1950-today) but it provides atmospheric variables with a high spatial resolution of $0.25°$. ERA5 assimilates surface observations, upper-air observations and satellite observations (referred as "full-input") using a 4D-Var scheme. ERA5 relies on the radiative forcing of CMIP5 including total solar irradiance, ozone, greenhouse gases and some aerosols including stratospheric sulfate aerosols. It takes sea-surface temperature and sea-ice cover as boundary conditions. A 10-member ensemble with reduced resolution is available, but we use the high resolution realisation of ERA5 which is referred to as the main reanalysis.

3 Method

Studying changes in LSC is carried out using atmospheric descriptors characterizing daily 500 hPa geopotential height fields. An existing weather pattern classification is also employed to consider changes in LSC characteristics that are specific to the main atmospheric influences.

3.1 Main atmospheric influences

We use the weather pattern classification of Garavaglia et al. (2010) from 1950 to 2019 to derive the main atmospheric influences affecting Western Europe. This classification into eight weather patterns was established to link daily rainfall field shapes over Southern France with synoptic situations. We aggregate the eight weather patterns into four atmospheric influences according to the origin of the air flow reaching the French Alps, as previously done in Blanc et al. (2021b) and Blanchet et al.

https://doi.org/10.5194/wcd-2021-69
Preprint. Discussion started: 19 October 2021

(2021b). We end up with four atmospheric influences: Atlantic circulations, Mediterranean circulations, Northeast circulations and Anticyclonic conditions (Fig. 1). The Atlantic, Mediterranean, Northeast and Anticyclonic influences respectively account for 37 %, 25 %, 9 % and 29 % of days between 1950 and 2019. Trends in occurrence of the main atmospheric influences are rather poor over this period, although a decreasing trend of the Northeast circulation is observed in spring and summer (Fig. 3 in Blanchet et al., 2021b).

3.2 Atmospheric descriptors

Changes in LSC characteristics are investigated using four atmospheric descriptors introduced in previous works (Blanc et al., 2021a; Blanchet et al., 2018; Blanchet and Creutin, 2020). These descriptors are based on daily 500 hPa geopotential height fields over Western Europe (rectangle in Fig. 1a). Three descriptors are based on analogy, that is on the comparison of daily geopotential height fields between each other. The analogy is based on the Teweles-Wobus score (Teweles and Wobus, 1954), which measures the similarity in shape between geopotential height fields using North-South and West-East gradients. As the geopotential shape defines the flow direction, we can interpret the analogy in Teweles-Wobus score as the analogy in flow direction. The Teweles-Wobus score between days t_k and $t_{k'}$ is given by:

$$TWS_{k,k'} = \frac{\sum_{(j,j')\in Adj} |(z_{jk} - z_{j'k}) - (z_{jk'} - z_{j'k'})|}{2\sum_{(j,j')\in Adj} \max(|z_{jk} - z_{j'k}|, |z_{jk'} - z_{j'k'}|)}, \quad (1)$$

where Adj ranges the set of adjacent grid points in horizontal and vertical directions in the region of study. A $TWS_{k,k'}$ of 0 means that day k and k' feature strictly identical flow directions. A $TWS_{k,k'}$ of 1 means that day k and k' feature strictly opposite flow directions. In practice, the TWS obtained in this study range between 0.04 and 0.88.

Figure 1b provides a schematic illustration of the three descriptors based on analogy in flow direction. The first descriptor is the celerity that is understood as the celerity of deformation of the geopotential. It measures the stationarity in flow direction between two consecutive days. It is defined for day t_k as the TWS between day t_k and day t_{k-1} (dotted arrow in Fig. 1b):

$$cel_k = TWS_{k-1,k}. \quad (2)$$

The lower the celerity, the more stationary the flow direction between two consecutive days.

The two other descriptors based on analogy are the singularity and relative singularity. They measure the way a flow direction is reproduced in the climatology. The singularity and relative singularity rely on the comparison of a given flow direction with its Q closest flow directions in the climatology, referred as its analogs. The singularity of day t_k is defined as the mean TWS between day t_k and its Q closest analog days (mean of solid arrows in Fig. 1b):

$$sing_k = \frac{1}{Q} \sum_{q\in A_k} TWS_{k,q}, \quad (3)$$

where $\mathcal{A}_k$ range the Q closest analogs of day t_k. A flow direction featuring a low singularity means that close flow directions are found in the climatology. The singularity cannot be directly related to the frequency of occurrence of a given flow direction since a geopotential shape is never perfectly reproduced ($TWS_{k,k'} > 0$). Very low singularities even appear to be rare in the

https://doi.org/10.5194/wcd-2021-69
Preprint. Discussion started: 19 October 2021

Weather and Climate Dynamics Discussions
Open Access
EGU

climatology, which means that the atmosphere spends much time exploring quite unseen patterns than very closely coming back to an already seen pattern (Blanc et al., 2021a; Blanchet and Creutin, 2020).

The relative singularity of day t_k is defined as the singularity normalized by the Teweles-Wobus score with the Qth closest analog day (mean of solid arrows normalized by the dashed arrow in Fig. 1b):

$$rsing_k = \frac{sing_k}{TWS_{k,(Q)}}. \quad (4)$$

The relative singularity measures the similarity of a given flow direction to its very close analogs in comparison to the farther analog. It measures in a way the degree of clustering of the closest flow directions. The relative singularity is closely related to the local dimension of Faranda et al. (2017a) although they employ an Euclidean distance instead of TWS. A flow direction featuring a low singularity and relative singularity is said to be almost similarly reproduced in the climatology, as close flow directions are found in the climatology (low singularity) but the closest flow directions tend to be even more resembling than usually (low relative singularity).

Blanchet and Creutin (2020) showed that the singularity and relative singularity are not very sensible to the exact number of days selected as analog in Eq. (3) and Eq. (4), and that the selection of the closest 0.5 % days was a reasonable choice to link LSC characteristics with 3-day precipitation in the Northern French Alps. The period 1950-2010 is considered for the search of analog, as it is the common period of 20CRv2c, ERA20C and ERA5. Therefore, we use in the rest of this study $Q = 111$ days.

The celerity, singularity and relative singularity are based on the TWS, which only focuses on geopotential shapes (that is on flow direction) whatever the range of geopotential heights, which governs the strength of the flow. Therefore we complement the three above analogy descriptors with the Maximum Pressure Difference (MPD) as fourth descriptor. The MPD of day t_k is defined as the range of geopotential heights over Western Europe (in meters):

$$MPD_k = \max_j(z_{jk}) - \min_j(z_{jk}). \quad (5)$$

The higher MPD_k, the larger the pressure difference between the low and the high pressure systems at day t_k, i.e. the more pronounced the centers of action over Western Europe for this day. Although it reflects a pressure difference, the MPD over Western Europe appears to be poorly related to NAO (Blanc et al., 2021b).

Overall, each result of the present paper are expressed per season. The four seasons are defined as December-January-February (winter), March-April-May (spring), June-July-August (summer), and September-October-November (autumn).

4 Results and Discussion

4.1 Past and Recent Evolution of Western Europe LSC from 1851 to 2010 at seasonal scale

The atmospheric descriptors are first employed to study the long-term evolution of Western Europe LSC over the period 1851-2010. As most of the descriptors rely on analogy in geopotential shapes, we start the analysis by checking whether the different reanalyses provide similar geopotential shapes over this period. Figure 2 shows the evolution of the Teweles

https://doi.org/10.5194/wcd-2021-69
Preprint. Discussion started: 19 October 2021

Wobus Score (TWS) between the daily geopotential height fields got from different reanalyses. ERA20C and ERA5 have been systematically interpolated on a coarser horizontal grid using a bilinear interpolation to allow the computation of crossed TWS between reanalyses. 20CRv2c grid is used to compare 20CRv2c, ERA20C and ERA5; ERA20C grid is used to compare ERA20C and ERA5. Recalling that a TWS score of 0 represents two identical geopotential shapes, we observe that differences in geopotential shapes between reanalyses are weaker after 1950 than before (20CRv2c, ERA20C) and that differences remain quite steady from 1950 to 2010 (20CRv2c, ERA20C, ERA5). Before 1950, larger differences are observed between 20CRv2c and ERA20C, especially at the beginning of the 20th century. Those differences in geopotential shapes are larger in summer and weaker in winter while spring and autumn feature a transitional behavior. As a reference, we add in Fig. 2 the TWS between days D and D-1 considered in Fig. 1b (celerity of 12 December 1978) that is equal to 0.28 and corresponds to the 69 % percentile of celerity. Differences in shape between ERA20C and 20CRv2c (in red) before 1950 are notable; they are close to a TWS of 0.28, which reflects significant differences in geopotential shapes (see the difference in geopotential shapes between days D and D-1 in Fig. 1b). Substantial differences in geopotential shapes are also observed between 20CRv2c members (in gray) from 1851 to 1880 but they always remain less pronounced than differences between reanalyses from 1900 to 1950. Furthermore, it is interesting to note the larger differences between reanalyses and members during both World Wars due to the weaker number of assimilated observations. Overall, the significant differences in geopotential shapes before 1950 combined with the non-stationarity of the differences along the 20th century may have implications on the long-term evolution of LSC obtained from 20CRv2c and ERA20C.

In order to better understand the differences in shape between 20CRv2c and ERA20C, we map in Fig. 3 the differences in 500 hPa geopotential height between 1970-2000 and 1900-1930 for the first member of 20CRv2c and for ERA20C. On the one hand, 20CRv2c shows mainly increases in the 500 hPa geopotential height between the two periods, with a more pronounced increase over Great Britain. On the other hand, ERA20C features an increase in the 500 hPa geopotential height mainly in Southern Europe while a decrease in observed in Northern and Northeastern Europe for almost every season. This decrease in 500 hPa geopotential height is located further North from Western Europe in winter (black rectangle). The increase in the meridional pressure gradient in ERA20C between the beginning and the end of the 20th century is in line with Bloomfield et al. (2018) who show an increase in the Arctic Oscillation from October to March in ERA20C. This increase is not observed in two other observation products; it appears to be explained in ERA20C by a larger sea-level pressure in the North Pole in 1900 that decreases along the 20th century, while no trend is observed over Northern Europe (Fig. 4 of Bloomfield et al., 2018). The latter is not necessarily in contradiction with our results since Bloomfield et al. (2018) study sea-level pressure while we study the 500 hPa geopotential height. At higher levels, this increase in meridional pressure gradient is consistent with Ménégoz et al. (2020) who show an increase in the westerly component of moisture flux over the Northern half of Europe using a regional climate model forced by ERA20C from 1902 to 2010 (Fig. 5 therein). It is also in line with Rohrer et al. (2019) showing an increasing storm track activity in ERA20C along the 20th century over the North Atlantic/European domain. Figure 3 therefore highlights that the spatial differences in geopotential shapes between ERA20 and 20CRv2c come out as a reinforcement of the meridional pressure gradient between 1900-1930 and 1970-2000 in ERA20C, that is not observed in 20CRv2c.

https://doi.org/10.5194/wcd-2021-69
Preprint. Discussion started: 19 October 2021

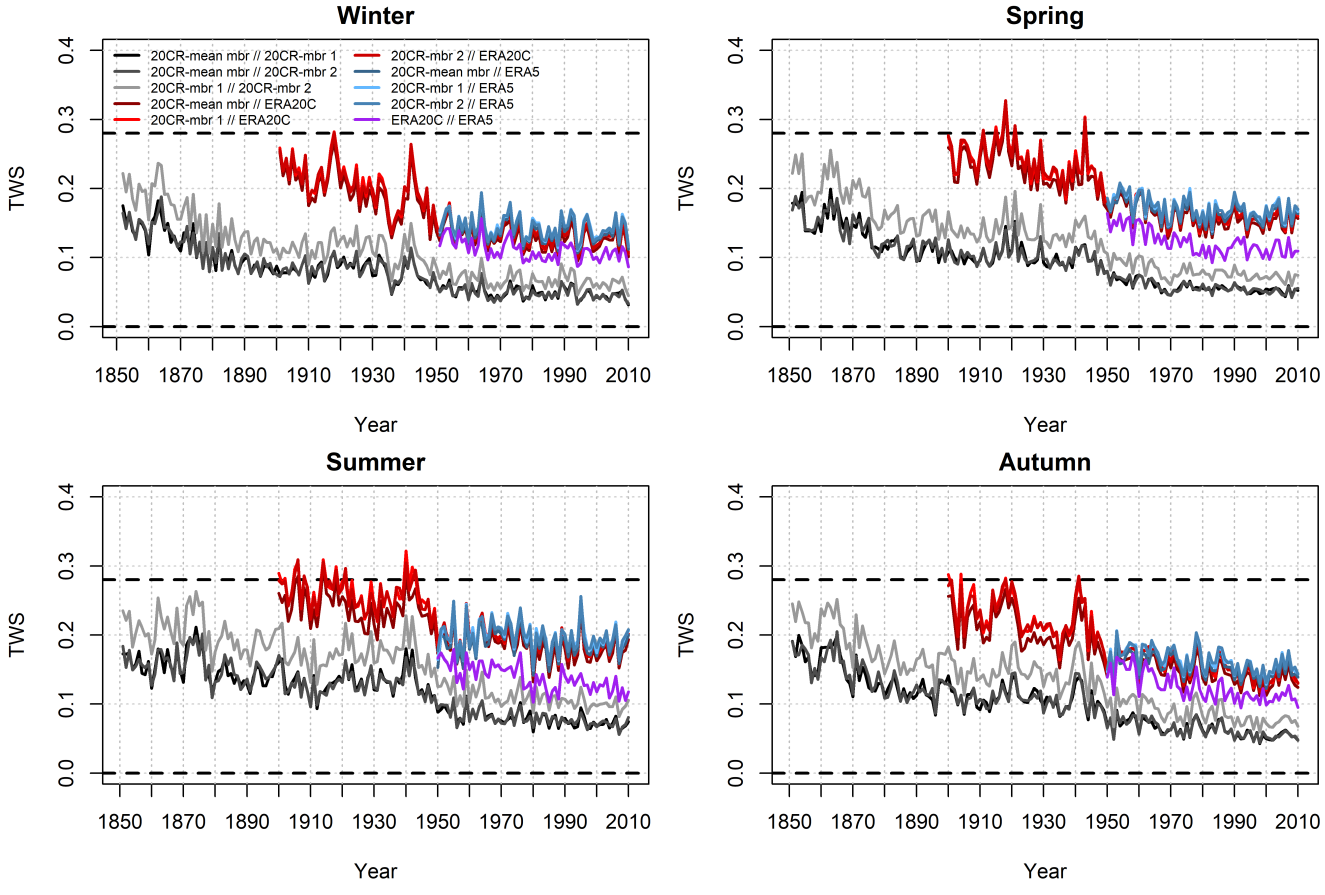

Figure 2. Evolution of the Teweles-Wobus Score (TWS) between the geopotential height fields from the different reanalyses over the period 1851-2010, per season. The black dotted lines show respectively the minimum TWS value (0) – when geopotential shapes are identical, and, for reference, the TWS between days D and D-1 in Fig. 1b ($TWS = 0.28$, corresponding to the 69 % percentile of celerity for the period 1950-2010 using ERA5).

https://doi.org/10.5194/wcd-2021-69
Preprint. Discussion started: 19 October 2021

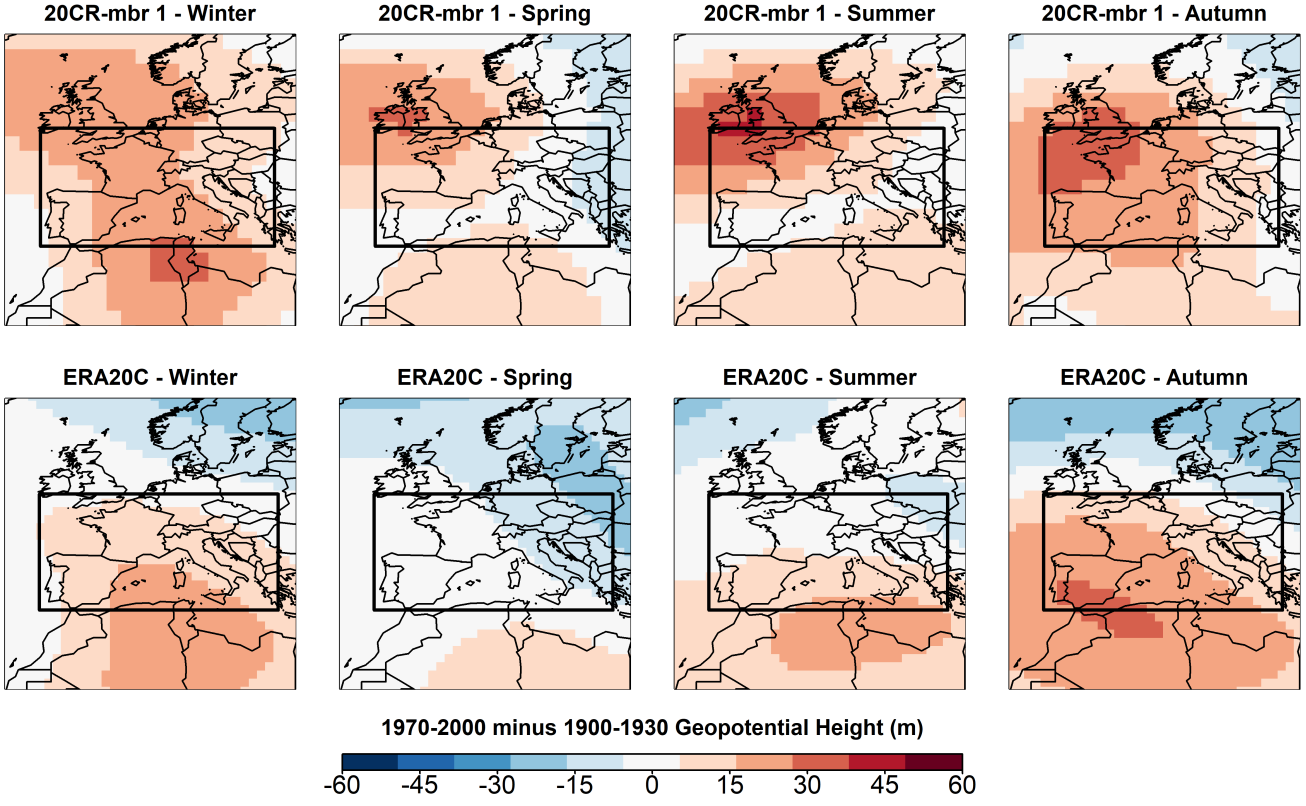

Figure 3. 500 hPa geopotential height difference (in meters) between 1970-2000 and 1900-1930 according to the first member of 20CRv2c (top) and ERA20C (bottom), per season. The Western Europe region over which the atmospheric descriptors are computed is represented by the black rectangle.

Finally, we plot the evolution of the four atmospheric descriptors over the period 1851-2010, considering a 5-year running average (Fig. 4). Overall, we observe a large interdecadal variability except for the celerity, that is broadly similar between the different reanalyses over the whole period. Except in summer, ERA5 produces larger values of celerity, singularity and relative singularity in comparison to the long-term reanalyses, as well as larger MPD values in every season (colored dots in 2010, Fig. 4). This result is consistent with Rohrer et al. (2018) who show that high-resolution reanalyses tend to produce larger cyclone intensities and higher cyclone center densities, while full-input reanalyses tend to produce more intense blockings. The higher spatial resolution of ERA5 as well as the assimilation of surface, upper-air and satellite observations generate more detailed geopotential shapes at 500 hPa, giving larger pressure differences (MPD) and weaker resemblances (celerity, singularity and relative singularity).

Over the period 1900-1950, major differences in descriptors trends are found between 20CRv2c and ERA20C. Differences are larger in summer and weaker in winter, as already observed for differences in geopotential shapes (Fig. 2). This result is in

https://doi.org/10.5194/wcd-2021-69
Preprint. Discussion started: 19 October 2021

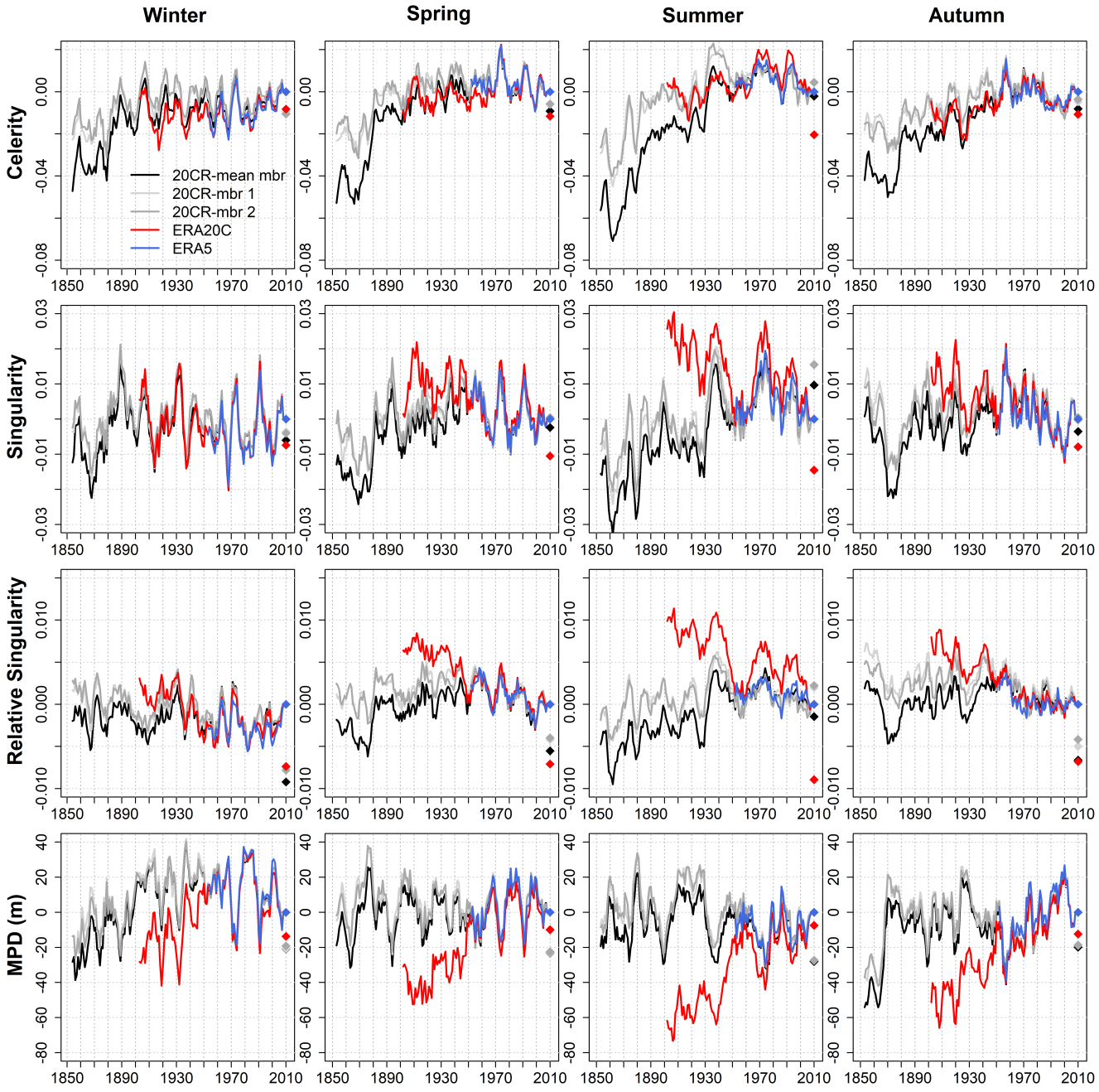

Figure 4. Evolution of the celerity, singularity, relative singularity and MPD per season over the period 1851-2010 for different reanalyses. A running average of 5 years is applied to allow a clearer visualisation. Time series are represented as anomalies according to the 2006-2010 average. The colored dots in 2010 indicate the differences in 2006-2010 average between ERA5 and the other reanalyses.

https://doi.org/10.5194/wcd-2021-69
Preprint. Discussion started: 19 October 2021

line with Rohrer et al. (2019), who show larger differences between 20CRv2c and ERA20C in summer than in winter regarding trends in the 500 hPa geopotential height variability over the North Atlantic/European domain (Fig. 4 therein). The differences in descriptor trends are considerable as they are clearly out of the range of the descriptor natural variability. Differences are more pronounced for the MPD, the relative singularity, and the singularity than for the celerity. ERA20C shows a strong trend at having more closely reproduced flow directions from 1900 to 1950, especially from spring to autumn (decreasing singularity and relative singularity). ERA20C also shows a strong trend at having more marked geopotential shapes from 1900 to 1950 (increasing MPD), in accordance with a reinforcement of the meridional pressure gradient (Fig. 3). These major differences in LSC trends between ERA20C and 20CRv2c are in line with several studies showing inconsistencies in wind speed trends between the two reanalyses before 1950 (Befort et al., 2016; Wohland et al., 2019). The assimilation of marine wind and the increasing number of associated observations in ERA20C is pointed as the main driver of the increasing wind speed in the reanalysis in the first half of the 20th century – a trend that is neither observed in the model-only integration ERA20CM nor in 20CRv2c which only assimilates surface pressure (Meucci et al., 2019; Wohland et al., 2019). Trends in wind speed may have impacted pressure at both sea level (Bloomfield et al., 2018) and higher elevations.

Substantial differences in trends are also found between the individual members and the mean member of 20CRv2c before 1950. Differences are also more pronounced from spring to autumn, and they are quite pronounced for the celerity. The mean member of 20CRv2c shows lower values of celerity from 1850 to 1880 together with a strong increase in celerity from 1880 to 1950, suggesting more stationary flow directions in the 19th century. This feature is however much less pronounced in 20CRv2c individual members. Notable differences between 20CRv2c mean and individual members are also observed before 1950 regarding the singularity and relative singularity. The lower number of assimilated data in the beginning of the 20CR reanalysis (see Fig. 2 of Wang et al., 2012) could explain i) the generation of smoother individual members, which allows for closer analogs and explains the systematically lower celerity and singularity in the beginning of the reanalysis, and ii) the larger differences in geopotential shapes between individual members, leading to a smoothed mean member and lower celerity, singularity and relative singularity in comparison to individual members. This is consistent with Rodrigues et al. (2018) who point the 20CRv2c ensemble mean as more suitable than the mean member to derive long-term trends in the dynamical properties of the North Atlantic circulation. This is reinforced by the fact that the two individual members mostly share the same evolution in LSC characteristics even with quite different geopotential shapes (Fig. 2). Furthermore, it is interesting to note that differences in MPD between individual and mean member are rather weak over the whole period, meaning that averaging individual members leads to smoother but not flatter geopotential shapes. This reflects that the location and the intensity of the centers of action in individual members of 20CRv2c are similar over the whole period of the reanalysis, while the other regions of the pressure fields are less constrained, and are thus more variable in shape. The fact that geopotential shapes are more marked in winter (larger MPD, see Fig. 7 of Blanc et al., 2021a) makes it easier to capture the main pattern of the circulation even with few assimilated observations, leading to weaker differences in geopotential shapes between individual and mean member in winter before 1950 (Fig. 2). Overall, the lower number of assimilated observations in the beginning of the 20CR reanalysis and the differences between individual and mean members make it difficult to explain the increasing celerity and singularity in the second half of the 19th century.

https://doi.org/10.5194/wcd-2021-69
Preprint. Discussion started: 19 October 2021

From 1950 to 2010, there is a good agreement between the different reanalyses. This result is in line with the weaker differences in geopotential shapes observed between reanalyses after 1950. We can note a negative trend in relative singularity in spring from 1950 to 2010, which is consistent with the decreasing local dimension of Rodrigues et al. (2018) and Faranda et al. (2019) over the North Atlantic, pointing to a decrease in the number of degrees of freedom around the atmospheric states. We can also note the increase in MPD in autumn, pointing to an increasing intensity of the centers of action over Western Europe from September to November.

To summarize, the interannual and interdecadal LSC variability is consistent between the three reanalyses, but substantial differences in LSC trends are observed before 1950 in 20CRv2c and ERA20C. ERA20C feature less marked and quite different geopotential shapes in comparison to 20CRv2c in the early 20th century, as well as a clear increase of the meridional pressure gradient until 1950. This result is consistent with the literature which shows that the pronounced trends in ERA20C might be driven by the increasing trend in the assimilated marine wind – a variable that is not assimilated in 20CRv2c. Furthermore, significant differences are also found between the geopotential shapes of 20CRv2c members before 1950, which is probably related the low number of assimilated data in the beginning of the reanalysis. The large differences in Western Europe LSC between long-term reanalyses hence make the study of LSC evolution difficult before 1950. In order to look in more details on the trends in LSC characteristics after 1950, we focus on the distributions of daily descriptors instead of their seasonal mean and we distinguish the main atmospheric influences affecting Western Europe.

4.2 Recent changes in Western Europe LSC from 1950 to 2019 at daily scale

We focus on the changes in Western Europe LSC from 1950 to 2019 thanks to ERA5. We take advantage of the atmospheric descriptors to study changes in the whole descriptor distribution at the daily scale, rather than only considering trends in mean descriptor values over a season as we did in Section 4.1. To do this, we separate the period 1950-2019 into two sub-periods of 35 years each and we look at the changes in descriptor distribution between the two sub-periods. Both Kolmogorov-Smirnoff and Anderson-Darling tests are carried out to detect significant differences in descriptor distribution at 5 % level. The significant differences in descriptor distribution and the sign of the difference in average descriptor value between the two sub-periods are summarized in Table 2. Considering the whole climatology, significant differences in descriptor distribution are found in summer and autumn for almost every atmospheric descriptor and in spring for the relative singularity. In summer and autumn, the significant differences in descriptor distribution share the same sign, pointing to a decreasing average celerity, singularity, relative singularity (summer only) and an increasing average MPD. Considering the main influences affecting Western Europe shows that the differences in descriptor distribution are not equally distributed over the different influences (Table 2). Northeast circulations show only one significant difference. Atlantic circulations and Anticyclonic conditions show more significant differences, that spread over the four seasons. Mediterranean circulations are definitely the most changing circulations with significant differences in every season but especially in summer and autumn. In the following, we focus in more details on the evolution of Anticyclonic conditions, Atlantic circulations and Mediterranean circulations.

https://doi.org/10.5194/wcd-2021-69
Preprint. Discussion started: 19 October 2021

		All	Atlantic	Mediterranean	Northeast	Anticyclonic
Winter	cel					
	sing		-	+*		-*
	rsing					
	MPD			-*	+*	+
Spring	cel			+		
	sing			+*		
	rsing	-*	-*			-
	MPD			-		
Summer	cel	-*	-*	-*		-*
	sing	-*		-*		
	rsing	-	-			
	MPD	+		+*		
Autumn	cel	-*		-		-*
	sing	-*		-*		
	rsing					
	MPD	+*	+	+*		

Table 2. Significant differences in descriptor distribution between the period 1985-2019 and the period 1950-1984 for every atmospheric influences (All), Atlantic circulations, Mediterranean circulations, Northeast circulations and Anticyclonic conditions. Differences are considered significant if the p-value of the Kolmogorov-Smirnoff test or of the Anderson-Darling test is lower than 5 %. Differences that are significant with both tests are marked with a *. The sign indicates whether the average descriptor value has increased (+) or decreased (-) from 1950-1984 to 1985-2019.

https://doi.org/10.5194/wcd-2021-69
Preprint. Discussion started: 19 October 2021

Weather and Climate Dynamics Discussions
Open Access
EGU

4.2.1 Anticyclonic conditions

Figure 5 shows the descriptor distribution of Anticyclonic conditions (boxplots) as well as the differences in descriptor densities between 1985-2019 (referred as the present period) and 1950-1984 (referred as the early period), per season. Over the present period, Anticyclonic conditions are associated with significantly lower celerities in summer and autumn. The increase in stationarity concerns Anticyclonic conditions below the 25 % percentile of celerity in summer and to a lesser extent Anticyclonic conditions below the 50 % percentile of celerity in autumn. In winter, Anticyclonic conditions are associated with lower singularities over the present period. This correspond to a strong decrease in the largest singularities (above 75 %), meaning that new anticyclonic patterns are less explored over the present period. Finally, Anticyclonic conditions are associated with more pronounced geopotential shapes in winter (larger MPD), the most pronounced geopotential shapes (above 75 %) getting even more pronounced in the present period. We study how these changes in LSC characteristics affecting Anticyclonic conditions are distributed spatially by comparing the 500 hPa geopotential height composites of the period 1950-1984 and 1985-2019, per season (Fig. 6). Reminding that Anticyclonic conditions are associated to high pressure anomalies centered over Ireland (Fig. 1a), the marked increase in 500 hPa geopotential height over Western Germany in spring suggests more eastward Anticyclonic blocking in the present period. In winter, the increase in 500 hPa geopotential height over the Atlantic up to Ireland suggests a reinforcement of the position of Anticyclonic blocking together with more intense blocking, in accordance with a decreasing singularity and an increasing MPD.

4.2.2 Atlantic circulations

Atlantic circulations feature a decreasing celerity in summer between the two sub-periods (Fig. 7). Atlantic circulations feature a decreasing relative singularity in spring and to a lesser extent in summer, pointing to more Atlantic circulations featuring more resembling closest flow directions than usually. Finally, Atlantic circulation feature slightly more pronounced centers of action in autumn (increasing MPD) and more closely reproduced flow directions in winter (decreasing singularity) over the present period. The increase in the reproducibility of Atlantic circulations in winter is associated with a marked increase in the most closely reproduced Atlantic circulations (below the 25 % percentile of singularity). This result is consistent with Yiou et al. (2018) who show that winter circulations over the North Atlantic tend to become more similar to already known patterns, with the dominant atmospheric patterns – mainly NAO+/zonal patterns – being trapped for longer times within the winter season. Looking at the spatial patterns of the differences, we observe that changes in 500 hPa height are quite weak from spring to autumn, although we can note a slight increase in the meridional pressure gradient in spring which could lead to a slight increase in the zonality of Atlantic circulations (Fig. 6). Winter definitely shows the largest differences with a marked increase in 500 hPa heights over Northern Italy and a decrease in the Northwest of Great Britain. According to the anomalies associated with Atlantic circulations (Fig. 1a), this pattern reflects i) a northward shift of the Atlantic storm track between the two sub-periods, and ii) an increasing southwest component of Atlantic circulations. The latter is consistent with a decreasing singularity, the least singular geopotential shapes for Western Europe featuring west-to-southwest flow directions (Fig. 6 in Blanc et al., 2021a).

https://doi.org/10.5194/wcd-2021-69
Preprint. Discussion started: 19 October 2021

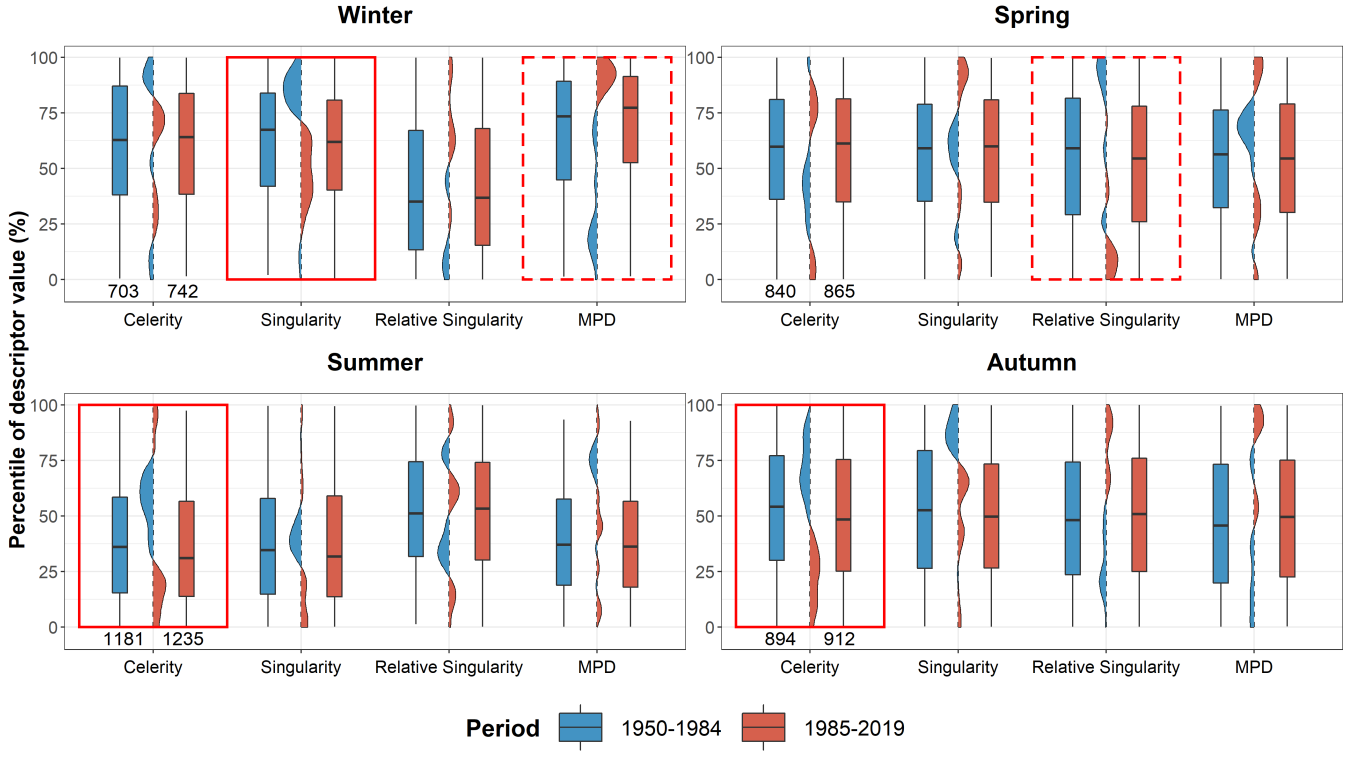

Figure 5. Boxplot of the daily celerity, singularity, relative singularity and MPD of Anticyclonic conditions for the two 35-year periods of 1950-1984 and 1985-2019, per season. Descriptor values are represented as percentiles to allow the representation of the four descriptors on the same axis. Percentiles are computed with respect to all days of 1950-2019 belonging to Anticyclonic conditions. The difference in density between the two sub-periods is shown between the boxplots. The range of the density that is colored in blue (respectively red) means that the considered descriptor shows more values within this range in the early (respectively present) period. The numbers in the bottom left of the graphs indicate the number of days considered in the early and present periods. A continuous red rectangle indicates the descriptor and season where the difference in distribution between the two sup-periods is significant according to both the Kolmogorov-Smirnov test and the Anderson-Darling test. A dashed red rectangle indicates significance with only one of the two tests. The difference is considered significant if the p-value of the test is lower than 5 %.

https://doi.org/10.5194/wcd-2021-69
Preprint. Discussion started: 19 October 2021

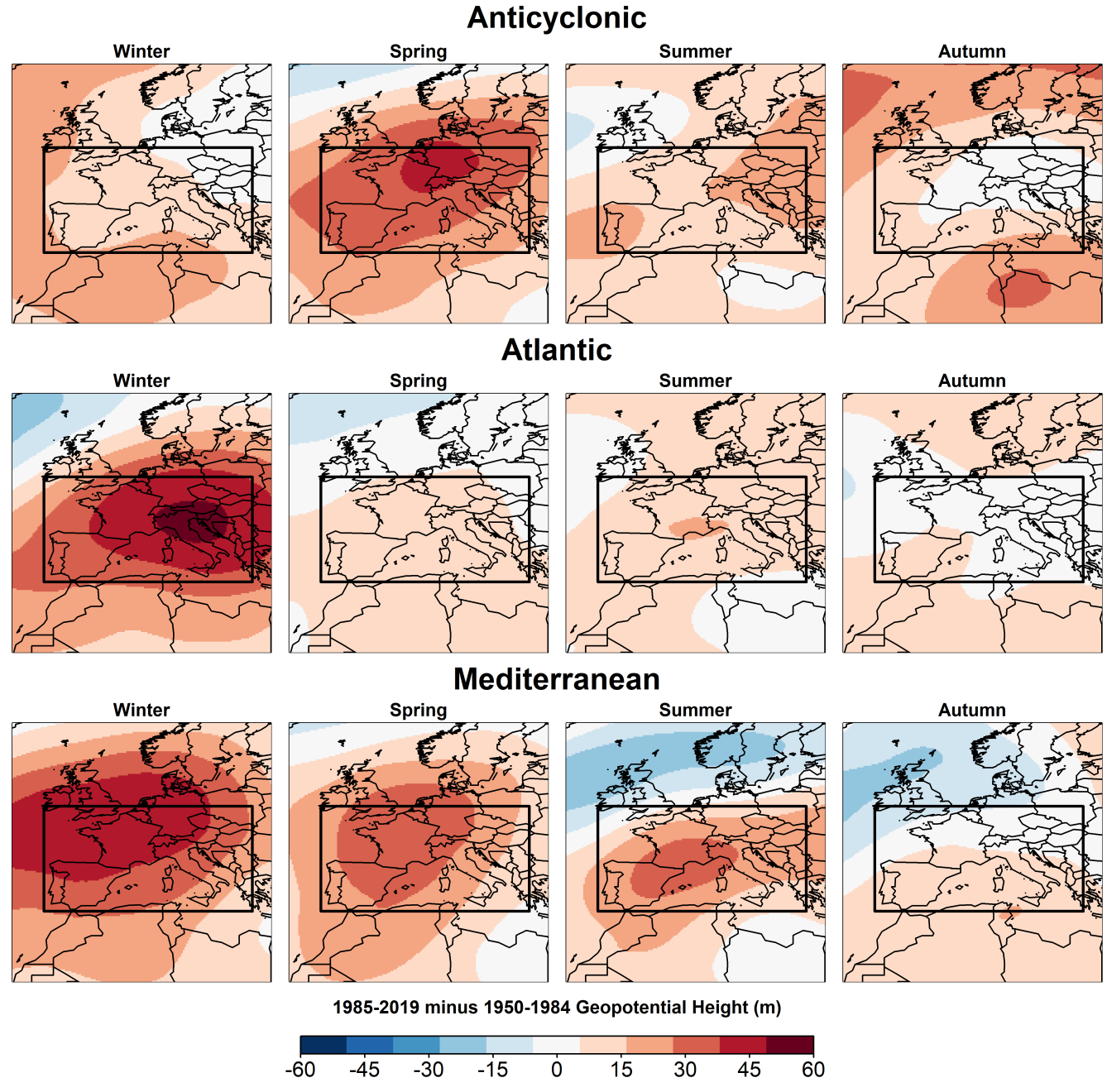

Figure 6. 500 hPa geopotential height difference (in meters) between 1985-2019 and 1950-1984 according to the ERA5 reanalysis for Anticyclonic conditions, Atlantic circulations and Mediterranean circulations, per season. The Western Europe region over which the atmospheric descriptors are computed is represented by the black rectangle. The maximum geopotential height difference displayed here reaches 60 m. This correspond to 30 % of the maximum anomalies of 200 m associated with the main atmospheric influences in Fig. 1a.

https://doi.org/10.5194/wcd-2021-69
Preprint. Discussion started: 19 October 2021

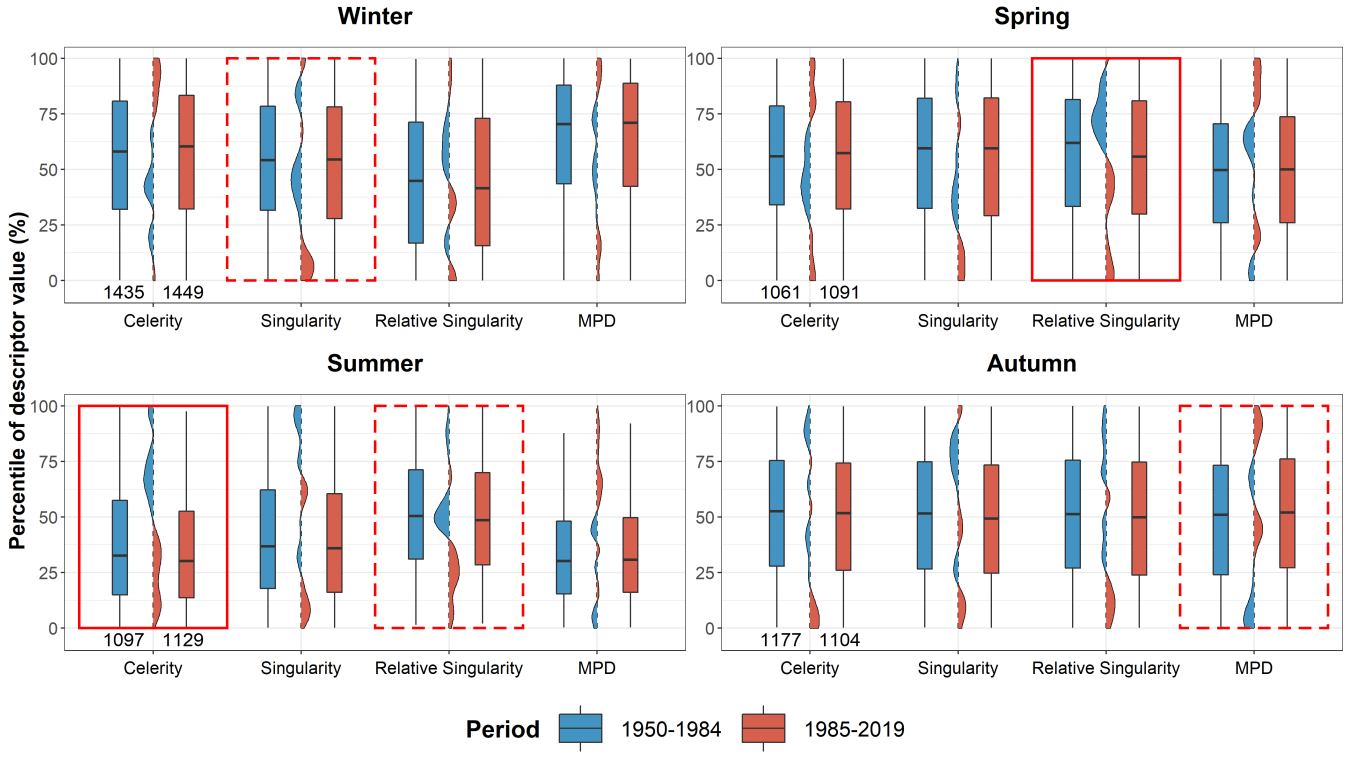

Figure 7. Same as Fig. 5, but for Atlantic circulations.

4.2.3 Mediterranean circulations

Mediterranean circulations feature clearly the largest differences in descriptor distribution between the early and the present period, with opposite differences across the seasons (Fig. 8). In summer and autumn, Mediterranean circulations become more stationary (lower celerity), more marked (larger MPD) and less singular in shape. These changes in LSC characteristics are more correlated in autumn than in summer, in so far as they affect more often the same days, as illustrated by the shift in the 2D descriptors densities of Fig. 9 showing combined lower celerity, lower singularity, lower relative singularity and larger MPD in autumn. Nevertheless, we can note that differences in 2D descriptors densities are only significant at 10 % level for the combination of the relative singularity and MPD. This shift in LSC characteristics in autumn corresponds to more than a doubling (from 0.7 % to 1.7 %) in the proportion of Mediterranean circulations featuring among the most stationary, the most closely reproduced and the most pronounced geopotential shapes (see the 10 % percentile in Fig. 10, right), and still a 30 % increase (from 7.9 % to 10.4 %) in the proportion of Mediterranean circulations featuring quite stationary, closely reproduced and pronounced geopotential shapes for Mediterranean circulations (see the 30 % percentile in Fig. 10, right). In summer, the shift affecting Mediterranean circulations concerns less extreme LSC characteristics, as shown by the 30 % increase for the 50 % percentile in Fig. 10 (left) and by the shift in density centers in Fig. 9.

https://doi.org/10.5194/wcd-2021-69
Preprint. Discussion started: 19 October 2021

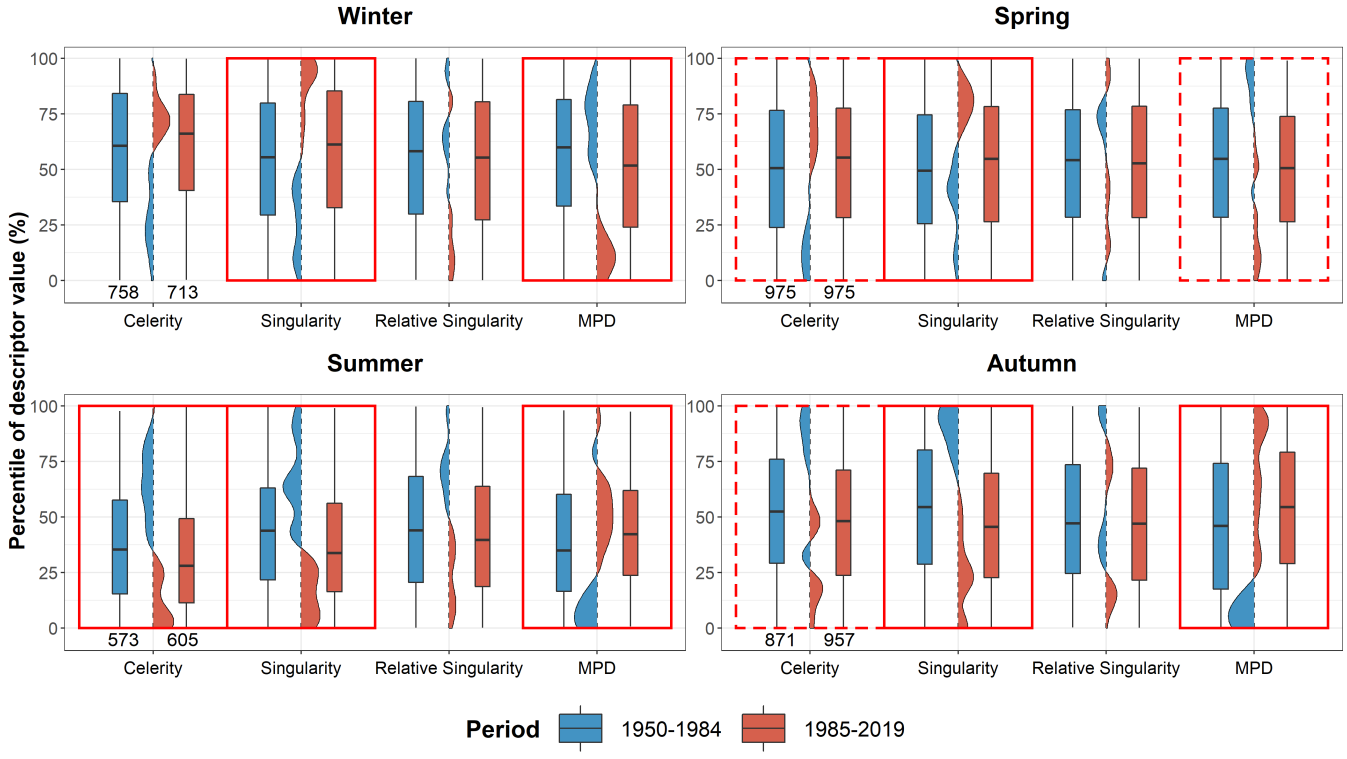

Figure 8. Same as Fig. 5, but for Mediterranean circulations.

In winter and spring, Mediterranean circulations tend to become more singular and less marked as well as less stationary (Fig. 8). The opposite patterns between autumn and winter changes could reflect a seasonal shift – the more marked, stationary and less singular Mediterranean circulations occurring in winter in the early period being shifted to autumn in the present period. The seasonal contrast of the differences in Mediterranean circulations is clearly visible in the maps of Fig. 6. Reminding that Mediterranean circulations are associated to low pressure anomalies over the near Atlantic (Fig. 1a), the large increase in 500 hPa geopotential height over the whole Northwestern Europe region in winter and to a lesser extent in spring confirms the weakening of Mediterranean circulations over the present period during these seasons. In summer and autumn, an opposite pattern is observed with a decreasing 500 hPa geopotential height over Northwestern Europe reaching further South in autumn, pointing to a reinforcing of Mediterranean circulations. The observed spatial patterns in summer and autumn – that is, an increasing pressure over Southern Europe and a decreasing pressure over Northwestern Europe – suggest an increasing zonality of Mediterranean flows. Blanc et al. (2021a) have shown that the singularity of Western Europe LSC is related to the zonality of the flow – the more zonal circulations being the more closely reproduced in the climatology. Here, the decreasing singularity of summer and autumn Mediterranean circulations together with the spatial patterns of the changes may suggest more frequent Southwestern flows and less frequent purely Southern flows at 500 hPa. This is fully consistent with the trends in summer 500 hPa circulation patterns over Europe for the period 1979-2013, showing an increasing occurrence of low pressure anomalies

https://doi.org/10.5194/wcd-2021-69
Preprint. Discussion started: 19 October 2021

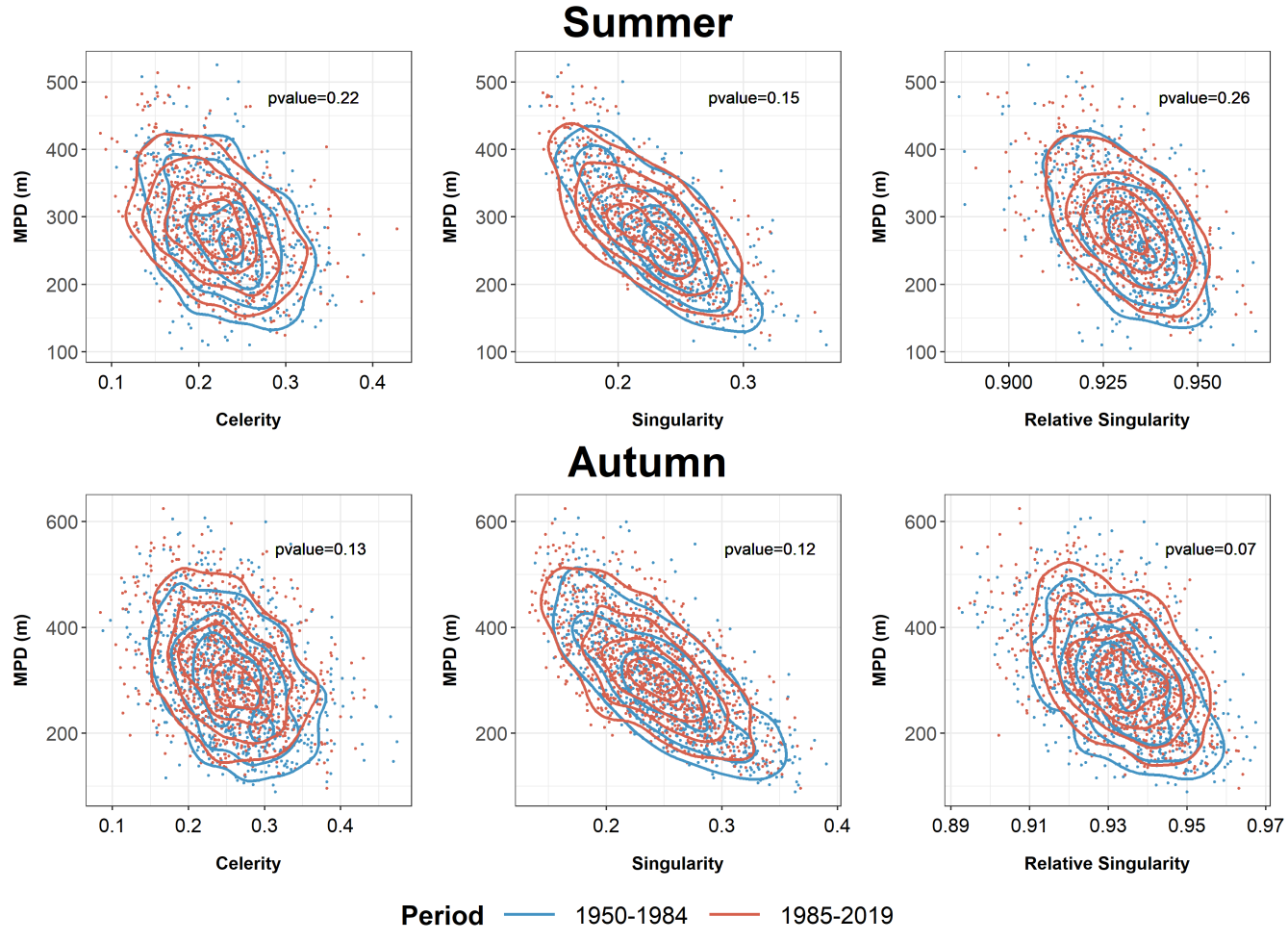

Figure 9. Scatterplot of the daily celerity, singularity, and relative singularity against the daily MPD of summer and autumn Mediterranean circulation for the two 34-year periods of 1950-1983 and 1984-2017. Contour lines indicate the density of points in the scatterplot. The pvalue of the Kernel density test is reported on each graph.

https://doi.org/10.5194/wcd-2021-69
Preprint. Discussion started: 19 October 2021

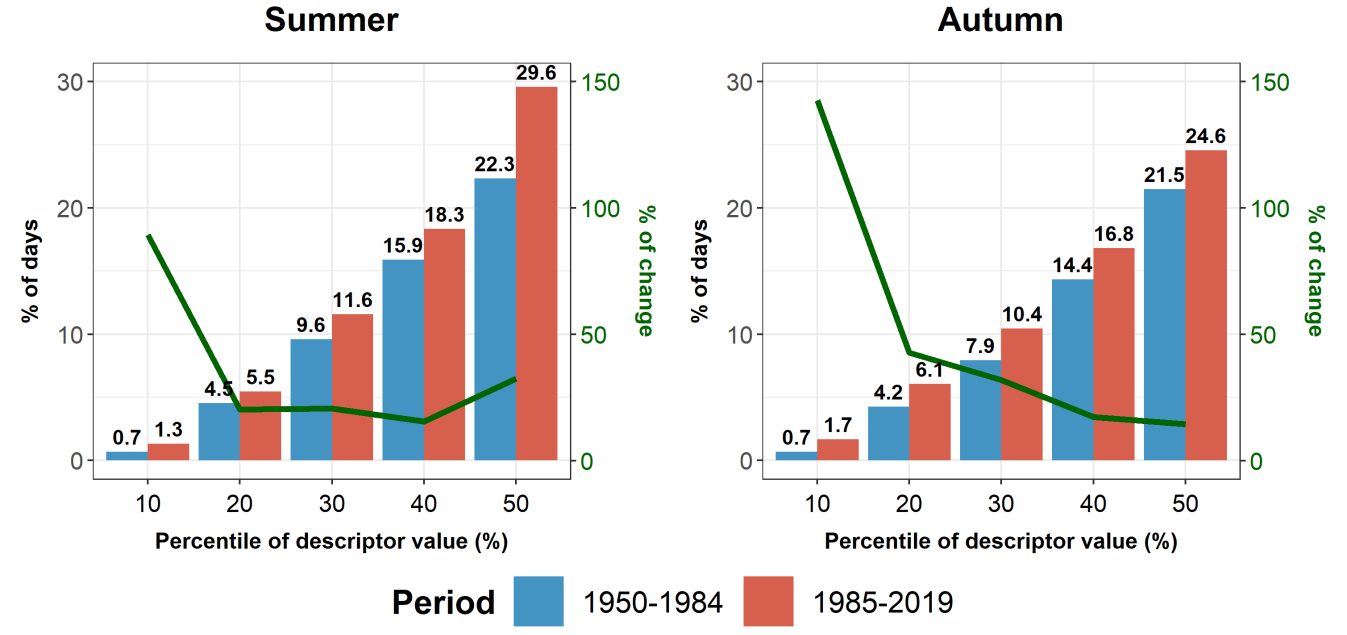

Figure 10. Percentage of summer and autumn Mediterranean circulations with combined celerity, singularity and relative singularity under a given percentile value per ($per = 10\%, 20\%, 30\%, 40\%, 50\%$) and MPD above its $100 - per$ percentile ($100 - per = 90\%, 80\%, 70\%, 60\%, 50\%$), for the two 35-year periods 1950-1984 and 1985-2019. For $per = 10\%$, this corresponds to Mediterranean circulations associated with flow directions that, compared to the climatology, are among the most stationary (celerity < 10% percentile), among the most closely reproduced in the climatology (singularity and relative singularity < 10% percentile) together with among the most pronounced centers of action (MPD > 90% percentile). The percentage of change in the relative occurrence of such days between the two periods is shown by the darkgreen line associated with the right y-axis. Summer (autumn) Mediterranean circulation represent 573 days (841 days) in the early period and 605 days (957 days) in the present period.

over the near Atlantic close to Ireland and a decreasing occurrence of low pressure anomalies centered over Northern Portugal (Extended Data Fig. 2 of Horton et al., 2015).

4.3 Potential impacts on local weather

The potential impacts of the observed changes in LSC on local weather can be discussed, both for weather variability and extremes. Focusing on weather variability, the increasing MPD in autumn for both Atlantic and Mediterranean circulations reflects more pronounced centers of action and suggests a stronger mean flow towards Western Europe. A previous study showed that autumn seasons associated with pronounced centers of action over Western Europe are associated with large precipitation amounts in the Northern French Alps (correlation of 0.68, see Fig. 4 of Blanc et al., 2021b). In this way, the

https://doi.org/10.5194/wcd-2021-69
Preprint. Discussion started: 19 October 2021

strengthening of the centers of action in autumn could induce an increase in autumn LSC-driven precipitation in the Northern French Alps.

Focusing on weather extremes, the increase in stationarity of Anticyclonic conditions in summer could have potential impacts on summer heatwaves, as the persistence of summer high pressure systems is a key parameter driving temperature extremes (Jézéquel et al., 2018; Riboldi et al., 2020). Regarding precipitation extremes, previous studies showed that Mediterranean circulations largely drive extreme daily precipitation in the Southwestern Alps in autumn (Blanchet et al., 2021b), and that the Mediterranean influence on extreme daily precipitation in autumn has been reinforced over the last 60 years (Fig. 4 therein). A considerable increase in extreme precipitation is also observed in the Mediterranean-influenced regions of the Southwestern Alps in autumn over the last 60 years – autumn being the season featuring the most extreme precipitations (Blanchet et al., 2021a). The combined increase in strength and stationarity of Mediterranean circulations in autumn – increasing the air flow toward a given region – together with an increasing humidity in a warmer air may increase the moisture flux, which is relevant to explain extreme precipitation magnitude and occurrence (Tramblay et al., 2012). Finally, previous studies showed that in winter and spring, the Mediterranean influence on extreme daily precipitation in the Southwestern Alps have significantly weakened over the last 60 years (Blanchet et al., 2021b). This is consistent with less pronounced and less stationary Mediterranean circulations in these seasons over the last 30 years.

5 Conclusions

We have studied the past evolution of Western Europe large-scale circulation based on the 500 hPa geopotential height fields using different reanalyses products. We employed several atmospheric descriptors that are mostly based on analogy and that allow a quantitative characterization of daily LSC.

We first focused on large-scale circulation evolution from 1851 to 2010 at seasonal scale. We showed major trend differences before 1950 between 20CRv2c and ERA20C, in accordance with the literature. The two reanalyses feature quite different geopotential shapes in the first half of the 20th century, especially from spring to autumn. ERA20C produces flatter geopotential shapes in the beginning of the 20th century and an increase in the meridional pressure gradient that is not observed in 20CRv2c. In 20CRv2c, the lower number of observations that are assimilated in the second half of the 19th century could lead to the generation of smoother geopotential shapes and may be responsible for the differences in geopotential shapes between the individual members, especially between 1850 and 1880. Overall, the differences in geopotential shapes in long-term reanalyses make it difficult to study long-term trends in Western Europe large-scale circulation.

We then focused on the changes in large-scale circulation after 1950 when the different reanalyses agree, using ERA5. The atmospheric descriptors have been combined to an existing weather pattern classification to study large-scale circulation changes in the main atmospheric influences affecting Western Europe. On the one hand, we have shown that little changes are observed for Northeast circulations. On the other hand, we have shown that winter Atlantic circulations tend to be more resembling to known Atlantic circulations over the last 30 years. Anticyclonic conditions associated with the most stationary geopotential shapes in summer are more frequent in the last 30 years than in the middle of the 20th century, which could have

https://doi.org/10.5194/wcd-2021-69
Preprint. Discussion started: 19 October 2021

implications for summer heatwaves. Mediterranean circulations featuring a marked flow and stationary flow directions that are closely reproduced in the climatology are more frequent over the last 30 years in autumn, which could impact autumn extreme precipitation over the Southwestern Alps.

The present work faces some limitations. The 70-year period considered from 1950 to 2019 allows the detection of changes in large-scale circulations that are relevant for local weather. However, this is still too short to deduce long-term trends knowing the large natural variability affecting large-scale circulation. Furthermore, the present study cannot assess whether the observed changes are a clear signal of climate change through anthropogenic forcing or a simple result of natural variability.

This article provides a view on the observed changes in regional large-scale circulation over the recent past. It opens the door to further studies quantifying the contribution of these changes to trends in local weather – including weather variability and extremes–, giving insights on the relevance of large-scale circulation to study future changes in local weather conditions.

Code and data availability. The R code can be requested by email from the corresponding author. The ERA5 reanalysis is available on the Copernicus Climate Data Store (https://cds.climate.copernicus.eu). The ERA20C reanalysis is available at https://apps.ecmwf.int/datasets/data/era20c-daily/levtype=sfc/type=an/. Informations on how to download the 20CRv2c reanalysis are available at https://psl.noaa.gov/data/gridded/data.20thC_ReanV2c.html. The weather pattern classification have been provided to the authors by Électricité de France for this research. They could be made available to other researchers under a specific research agreement. Requests should be sent to dtg-demande-donnees-hydro@edf.fr.

Author contributions. AB: data curation; formal analysis; investigation; methodology; software; visualization; writing-original draft preparation; writing-review and editing. JB: funding acquisition; methodology; project administration; supervision; validation; writing-review and editing. JDC: funding acquisition; methodology; project administration; validation.

Competing interests. The authors declare that they have no conflict of interest.

Acknowledgements. This study is part of a collaboration between the University Grenoble Alpes and Grenoble Alpes Métropole, the metropolitan authority of the Grenoble conurbation (deliberation 12 of the Metropolitan Council of May 27, 2016).

https://doi.org/10.5194/wcd-2021-69
Preprint. Discussion started: 19 October 2021

Weather and Climate Dynamics Discussions
Open Access
EGU

References

Auer, I., Böhm, R., Jurkovic, A., Lipa, W., Orlik, A., Potzmann, R., Schöner, W., Ungersböck, M., Matulla, C., Briffa, K., Jones, P., Efthymiadis, D., Brunetti, M., Nanni, T., Maugeri, M., Mercalli, L., Mestre, O., Moisselin, J.-M., Begert, M., Müller-Westermeier, G., Kveton, V., Bochnicek, O., Stastny, P., Lapin, M., Szalai, S., Szentimrey, T., Cegnar, T., Dolinar, M., Gajic-Capka, M., Zaninovic, K., Majstorovic, Z., and Nieplova, E.: HISTALP—historical instrumental climatological surface time series of the Greater Alpine Region, International Journal of Climatology, 27, 17–46, https://doi.org/10.1002/joc.1377, 2007.

Barnston, A. G. and Livezey, R. E.: Classification, Seasonality and Persistence of Low-Frequency Atmospheric Circulation Patterns, Monthly Weather Review, 115, 1083–1126, https://doi.org/10.1175/1520-0493(1987)115<1083:CSAPOL>2.0.CO;2, 1987.

Bartolini, E., Claps, P., and D'Odorico, P.: Interannual variability of winter precipitation in the European Alps: relations with the North Atlantic Oscillation., Hydrology and Earth System Sciences, 13, 17–25, https://doi.org/10.5194/hess-13-17-2009, 2009.

Befort, D. J., Wild, S., Kruschke, T., Ulbrich, U., and Leckebusch, G. C.: Different long-term trends of extra-tropical cyclones and windstorms in ERA-20C and NOAA-20CR reanalyses, Atmospheric Science Letters, 17, 586–595, https://doi.org/10.1002/asl.694, 2016.

Beniston, M.: Mountain Climates and Climatic Change: An Overview of Processes Focusing on the European Alps, pure and applied geophysics, 162, 1587–1606, https://doi.org/10.1007/s00024-005-2684-9, 2005.

Blanc, A., Blanchet, J., and Creutin, J.-D.: Characterizing large-scale circulations driving extreme precipitation in the Northern French Alps, International Journal of Climatology, https://doi.org/10.1002/joc.7254, 2021a.

Blanc, A., Blanchet, J., and Creutin, J.-D.: Linking Large-Scale Circulation Descriptors to Precipitation Variability in the Northern French Alps, Geophysical Research Letters, 48, e2021GL093 649, https://doi.org/10.1029/2021GL093649, 2021b.

Blanchet, J. and Creutin, J.-D.: Explaining Rainfall Accumulations over Several Days in the French Alps Using Low-Dimensional Atmospheric Predictors Based on Analogy, Journal of Applied Meteorology and Climatology, 59, 237–250, https://doi.org/10.1175/JAMC-D-19-0112.1, 2020.

Blanchet, J., Stalla, S., and Creutin, J.-D.: Analogy of multiday sequences of atmospheric circulation favoring large rainfall accumulation over the French Alps, Atmospheric Science Letters, 19, e809, https://doi.org/10.1002/asl.809, 2018.

Blanchet, J., Blanc, A., and Creutin, J.-D.: Explaining recent trends in extreme precipitation in the Southwestern Alps by changes in atmospheric influences, Weather and Climate Extremes, 33, 100 356, https://doi.org/10.1016/j.wace.2021.100356, 2021a.

Blanchet, J., Creutin, J.-D., and Blanc, A.: Retreating winter and strengthening autumn Mediterranean influence on extreme precipitation in the Southwestern Alps over the last 60 years, Environmental Research Letters, 16, 034 056, https://doi.org/10.1088/1748-9326/abb5cd, 2021b.

Bloomfield, H. C., Shaffrey, L. C., Hodges, K. I., and Vidale, P. L.: A critical assessment of the long-term changes in the wintertime surface Arctic Oscillation and Northern Hemisphere storminess in the ERA20C reanalysis, Environmental Research Letters, 13, 094 004, https://doi.org/10.1088/1748-9326/aad5c5, 2018.

Boé, J. and Terray, L.: A Weather-Type Approach to Analyzing Winter Precipitation in France: Twentieth-Century Trends and the Role of Anthropogenic Forcing, Journal of Climate, 21, 3118–3133, https://doi.org/10.1175/2007JCLI1796.1, 2008.

Brönnimann, S., Frigerio, L., Schwander, M., Rohrer, M., Stucki, P., and Franke, J.: Causes of increased flood frequency in central Europe in the 19th century, Climate of the Past, 15, 1395–1409, https://doi.org/10.5194/cp-15-1395-2019, 2019.

Brunner, L., Hegerl, G. C., and Steiner, A. K.: Connecting Atmospheric Blocking to European Temperature Extremes in Spring, Journal of Climate, 30, 585 – 594, https://doi.org/10.1175/JCLI-D-16-0518.1, 2017.

https://doi.org/10.5194/wcd-2021-69
Preprint. Discussion started: 19 October 2021

Buehler, T., Raible, C. C., and Stocker, T. F.: The relationship of winter season North Atlantic blocking frequencies to extreme cold or dry spells in the ERA-40, Tellus A: Dynamic Meteorology and Oceanography, 63, 174–187, https://doi.org/10.1111/j.1600-0870.2010.00492.x, 2011.

Compo, G. P., Whitaker, J. S., Sardeshmukh, P. D., Matsui, N., Allan, R. J., Yin, X., Gleason, B. E., Vose, R. S., Rutledge, G., Bessemoulin, P., Brönnimann, S., Brunet, M., Crouthamel, R. I., Grant, A. N., Groisman, P. Y., Jones, P. D., Kruk, M. C., Kruger, A. C., Marshall, G. J., Maugeri, M., Mok, H. Y., Nordli, O., Ross, T. F., Trigo, R. M., Wang, X. L., Woodruff, S. D., and Worley, S. J.: The Twentieth Century Reanalysis Project, Quarterly Journal of the Royal Meteorological Society, 137, 1–28, https://doi.org/10.1002/qj.776, 2011.

Faranda, D., Messori, G., and Yiou, P.: Dynamical proxies of North Atlantic predictability and extremes, Scientific reports, 7, 41 278, https://doi.org/10.1038/srep41278, 2017a.

Faranda, D., Alvarez-Castro, M. C., Messori, G., Rodrigues, D., and Yiou, P.: The hammam effect or how a warm ocean enhances large scale atmospheric predictability, Nature communications, 10, 1–7, https://doi.org/10.1038/s41467-019-09305-8, 2019.

Folland, C. K., Knight, J., Linderholm, H. W., Fereday, D., Ineson, S., and Hurrell, J. W.: The Summer North Atlantic Oscillation: Past, Present, and Future, Journal of Climate, 22, 1082–1103, https://doi.org/10.1175/2008JCLI2459.1, 2009.

Garavaglia, F., Gailhard, J., Paquet, E., Lang, M., Garçon, R., and Bernardara, P.: Introducing a rainfall compound distribution model based on weather patterns sub-sampling, Hydrology and Earth System Sciences, 14, 951–964, https://doi.org/10.5194/hess-14-951-2010, 2010.

Giannakaki, P. and Martius, O.: Synoptic-scale flow structures associated with extreme precipitation events in northern Switzerland, International Journal of Climatology, 36, 2497–2515, https://doi.org/10.1002/joc.4508, 2016.

Glur, L., Wirth, S., Büntgen, U., Gilli, A., Haug, G., Schär, C., Beer, J., and Anselmetti, F.: Frequent floods in the European Alps coincide with cooler periods of the past 2500 years, Scientific reports, 3, 2770, https://doi.org/10.1038/srep02770, 2013.

Grams, C. M., Binder, H., Pfahl, S., Piaget, N., and Wernli, H.: Atmospheric processes triggering the central European floods in June 2013, Natural Hazards and Earth System Sciences, 14, 1691–1702, https://doi.org/10.5194/nhess-14-1691-2014, 2014.

Hersbach, H., Bell, B., Berrisford, P., Hirahara, S., Horányi, A., Muñoz-Sabater, J., Nicolas, J., Peubey, C., Radu, R., Schepers, D., Simmons, A., Soci, C., Abdalla, S., Abellan, X., Balsamo, G., Bechtold, P., Biavati, G., Bidlot, J., Bonavita, M., De Chiara, G., Dahlgren, P., Dee, D., Diamantakis, M., Dragani, R., Flemming, J., Forbes, R., Fuentes, M., Geer, A., Haimberger, L., Healy, S., Hogan, R. J., Hólm, E., Janisková, M., Keeley, S., Laloyaux, P., Lopez, P., Lupu, C., Radnoti, G., de Rosnay, P., Rozum, I., Vamborg, F., Villaume, S., and Thépaut, J.-N.: The ERA5 global reanalysis, Quarterly Journal of the Royal Meteorological Society, 146, 1999–2049, https://doi.org/10.1002/qj.3803, 2020.

Horton, D., Johnson, N., Singh, D., Swain, D., Rajaratnam, B., and Diffenbaugh, N.: Contribution of changes in atmospheric circulation patterns to extreme temperature trends, Nature, 522, 465–9, https://doi.org/10.1038/nature14550, 2015.

Horton, P., Jaboyedoff, M., Metzger, R., Obled, C., and Marty, R.: Spatial relationship between the atmospheric circulation and the precipitation measured in the western Swiss Alps by means of the analogue method, Natural Hazards and Earth System Sciences, 12, 777– 784, https://doi.org/10.5194/nhess-12-777-2012, 2012.

Hurrell, J. W.: Decadal Trends in the North Atlantic Oscillation: Regional Temperatures and Precipitation, Science, 269, 676–679, https://doi.org/10.1126/science.269.5224.676, 1995.

Iannuccilli, M., Bartolini, G., Betti, G., Crisci, A., Grifoni, D., Gozzini, B., Messeri, A., Morabito, M., Tei, C., Torrigiani Malaspina, T., Vallorani, R., and Messeri, G.: Extreme precipitation events and their relationships with circulation types in Italy, International Journal of Climatology, n/a, https://doi.org/10.1002/joc.7109, 2021.

https://doi.org/10.5194/wcd-2021-69
Preprint. Discussion started: 19 October 2021

James, P., Stohl, A., Spichtinger, N., Eckhardt, S., and Forster, C.: Climatological aspects of the extreme European rainfall of August 2002 and a trajectory method for estimating the associated evaporative source regions, Natural Hazards and Earth System Science, 4, 733–746, https://hal.archives-ouvertes.fr/hal-00299223, 2004.

Jézéquel, A., Yiou, P., and Radanovics, S.: Role of circulation in European heatwaves using flow analogues, Climate Dynamics, 50, 1145–1159, https://doi.org/10.1007/s00382-017-3667-0, 2018.

Jézéquel, A., Yiou, P., Radanovics, S., and Vautard, R.: Analysis of the Exceptionally Warm December 2015 in France Using Flow Analogues, Bulletin of the American Meteorological Society, 99, S76–S79, https://doi.org/10.1175/BAMS-D-17-0103.1, 2017.

Kašpar, M. and Müller, M.: Combinations of large-scale circulation anomalies conducive to precipitation extremes in the Czech Republic, Atmospheric Research, 138, 205 – 212, https://doi.org/https://doi.org/10.1016/j.atmosres.2013.11.014, 2014.

Kotsias, G., Lolis, C., Hatzianastassiou, N., Levizzani, V., and Bartzokas, A.: On the connection between large-scale atmospheric circulation and winter GPCP precipitation over the Mediterranean region for the period 1980-2017, Atmospheric Research, p. 104714, https://doi.org/https://doi.org/10.1016/j.atmosres.2019.104714, 2019.

Lenggenhager, S. and Martius, O.: Atmospheric blocks modulate the odds of heavy precipitation events in Europe, Climate Dynamics, https://doi.org/10.1007/s00382-019-04779-0, 2019.

Mastrantonas, N., Herrera-Lormendez, P., Magnusson, L., Pappenberger, F., and Matschullat, J.: Extreme precipitation events in the Mediterranean: Spatiotemporal characteristics and connection to large-scale atmospheric flow patterns, International Journal of Climatology, 41, 2710–2728, https://doi.org/https://doi.org/10.1002/joc.6985, 2021.

Ménégoz, M., Valla, E., Jourdain, N. C., Blanchet, J., Beaumet, J., Wilhelm, B., Gallée, H., Fettweis, X., Morin, S., and Anquetin, S.: Contrasting seasonal changes in total and intense precipitation in the European Alps from 1903 to 2010, Hydrology and Earth System Sciences Discussions, pp. 1–37, 2020.

Messori, G., Caballero, R., and Faranda, D.: A dynamical systems approach to studying midlatitude weather extremes, Geophysical Research Letters, 44, 3346–3354, https://doi.org/10.1002/2017GL072879, 2017.

Meucci, A., Young, I. R., Aarnes, O. J., and Breivik, O.: Comparison of Wind Speed and Wave Height Trends from Twentieth-Century Models and Satellite Altimeters, Journal of Climate, 33, 611–624, https://doi.org/10.1175/JCLI-D-19-0540.1, 2019.

Müller, M., Kašpar, M., Řezáčová, D., and Sokol, Z.: Extremeness of meteorological variables as an indicator of extreme precipitation events, Atmospheric Research, 92, 308 – 317, https://doi.org/https://doi.org/10.1016/j.atmosres.2009.01.010, 7th International Workshop on Precipitation in Urban Areas, 2009.

Pfahl, S. and Wernli, H.: Quantifying the relevance of atmospheric blocking for co-located temperature extremes in the Northern Hemisphere on (sub-)daily time scales, Geophysical Research Letters, 39, https://doi.org/10.1029/2012GL052261, 2012.

Plaut, G. and Simonnet, E.: Large-scale circulation classification, weather regimes, and local climate over France, the Alps and Western Europe, Climate Research - CLIMATE RES, 17, 303–324, https://doi.org/10.3354/cr017303, 2001.

Plaut, G., Schuepbach, E., and Marut, D.: Heavy precipitation events over a few Alpine sub-regions and the links with large-scale circulation, 1971-1995, Climate Research, 17, 285–302, https://doi.org/10.3354/cr017285, 2001.

Poli, P., Hersbach, H., Dee, D. P., Berrisford, P., Simmons, A. J., Vitart, F., Laloyaux, P., Tan, D. G. H., Peubey, C., Thépaut, J.-N., Trémolet, Y., Hólm, E. V., Bonavita, M., Isaksen, L., and Fisher, M.: ERA-20C: An Atmospheric Reanalysis of the Twentieth Century, Journal of Climate, 29, 4083–4097, https://doi.org/10.1175/JCLI-D-15-0556.1, 2016.

Quadrelli, R., Lazzeri, M., Cacciamani, C., and Tibaldi, S.: Observed winter Alpine precipitation variability and links with large-scale circulation patterns, Climate Research - CLIMATE RES, 17, 275–284, https://doi.org/10.3354/cr017275, 2001.

https://doi.org/10.5194/wcd-2021-69
Preprint. Discussion started: 19 October 2021

Riboldi, J., Lott, F., D'Andrea, F., and Rivière, G.: On the Linkage Between Rossby Wave Phase Speed, Atmospheric Blocking, and Arctic Amplification, Geophysical Research Letters, 47, e2020GL087 796, https://doi.org/10.1029/2020GL087796, e2020GL087796 10.1029/2020GL087796, 2020.

Rodrigues, D., Alvarez-Castro, M. C., Messori, G., Yiou, P., Robin, Y., and Faranda, D.: Dynamical properties of the North Atlantic atmospheric circulation in the past 150 years in CMIP5 models and the 20CRv2c Reanalysis, Journal of Climate, 31, 6097–6111, https://doi.org/10.1175/JCLI-D-17-0176.1, 2018.

Rohrer, M., Brönnimann, S., Martius, O., Raible, C., Wild, M., and Compo, G.: Representation of Extratropical Cyclones, Blocking Anticyclones, and Alpine Circulation Types in Multiple Reanalyses and Model Simulations, Journal of Climate, 31, 3009–3031, https://doi.org/10.1175/JCLI-D-17-0350.1, 2018.

Rohrer, M., Brönnimann, S., Martius, O., Raible, C. C., and Wild, M.: Decadal variations of blocking and storm tracks in centennial reanalyses, Tellus A: Dynamic Meteorology and Oceanography, 71, 1586 236, https://doi.org/10.1080/16000870.2019.1586236, 2019.

Scherrer, S. C. and Appenzeller, C.: Swiss Alpine snow pack variability: major patterns and links to local climate and large-scale flow, Climate Research, 32, 187–199, 2006.

Scherrer, S. C., Begert, M., Croci-Maspoli, M., and Appenzeller, C.: Long series of Swiss seasonal precipitation: regionalization, trends and influence of large-scale flow, International Journal of Climatology, 36, 3673–3689, https://doi.org/10.1002/joc.4584, 2016.

Stucki, P., Rickli, R., Brönnimann, S., Martius, O., Wanner, H., Grebner, D., and Luterbacher, J.: Weather patterns and hydro-climatological precursors of extreme floods in Switzerland since 1868, Meteorologische Zeitschrift, 21, 531–550, https://doi.org/10.1127/0941-2948/2012/368, 2012.

Teweles, S. and Wobus, H. B.: Verification of Prognostic Charts, Bulletin of the American Meteorological Society, 35, 455–463, https://doi.org/10.1175/1520-0477-35.10.455, 1954.

Tramblay, Y., Neppel, L., Carreau, J., and Sanchez-Gomez, E.: Extreme value modelling of daily areal rainfall over Mediterranean catchments in a changing climate, Hydrological Processes, 26, 3934–3944, https://doi.org/10.1002/hyp.8417, 2012.

Vautard, R. and Yiou, P.: Control of recent European surface climate change by atmospheric flow, Geophysical Research Letters, 36, https://doi.org/10.1029/2009GL040480, 2009.

Wang, X., Feng, Y., Compo, G., Swail, V., Zwiers, F., Allan, R., and Sardesmukh, P.: Trends and low frequency variability of extra-tropical cyclone activity in the ensemble of Twentieth Century Reanalysis, Climate Dynamics, 40, 2775–2800, https://doi.org/10.1007/s00382-012-1450-9, 2012.

Wirth, S. B., Glur, L., Gilli, A., and Anselmetti, F. S.: Holocene flood frequency across the Central Alps – solar forcing and evidence for variations in North Atlantic atmospheric circulation, Quaternary Science Reviews, 80, 112–128, https://doi.org/10.1016/j.quascirev.2013.09.002, 2013.

Wohland, J., Omrani, N.-E., Witthaut, D., and Keenlyside, N. S.: Inconsistent Wind Speed Trends in Current Twentieth Century Reanalyses, Journal of Geophysical Research: Atmospheres, 124, 1931–1940, https://doi.org/10.1029/2018JD030083, 2019.

Yiou, P., Cattiaux, J., Ribes, A., Vautard, R., and Vrac, M.: Recent Trends in the Recurrence of North Atlantic Atmospheric Circulation Patterns, Complexity, 2018, 1–8, https://doi.org/10.1155/2018/3140915, 2018.